Special Section: State of the Field: Advances in Neuroimaging from the 2017 Alzheimer's Imaging Consortium

The personalized Alzheimer's disease cortical thickness index predicts likely pathology and clinical progression in mild cognitive impairment

Annie M. Racine[a,b,c], Michael Brickhouse[c], David A. Wolk[d], Bradford C. Dickerson[b,c,e,f,*], For the Alzheimer's Disease Neuroimaging Initiative[1]

[a]Aging Brain Center, Institute for Aging Research, Hebrew SeniorLife, Boston, MA, USA
[b]Harvard Medical School, Boston, MA, USA
[c]Frontotemporal Disorders Unit, Department of Neurology, Massachusetts General Hospital, Boston, MA, USA
[d]Department of Neurology, Perelman School of Medicine, and Penn Memory Center, University of Pennsylvania, Philadelphia, PA, USA
[e]Massachusetts Alzheimer's Disease Research Center, Massachusetts General Hospital, Boston, MA, USA
[f]Athinoula A. Martinos Center for Biomedical Imaging, Massachusetts General Hospital, Boston, MA, USA

Abstract

Introduction: An Alzheimer's disease (AD) biomarker adjusted for age-related brain changes should improve specificity for AD-related pathological burden.

Methods: We calculated a brain-age-adjusted "personalized AD cortical thickness index" (pADi) in mild cognitive impairment patients from the Alzheimer's Disease Neuroimaging Initiative. We performed receiver operating characteristic analysis for discrimination between patients with and without cerebrospinal fluid evidence of AD and logistic regression in an independent sample to determine if a dichotomized pADi predicted conversion to AD dementia.

Results: Receiver operating characteristic area under the curve was 0.69 and 0.72 in the two samples. Three empirical methods identified the same cut-point for pADi in the discovery sample. In the validation sample, 83% of pADi+ mild cognitive impairment patients were cerebrospinal fluid AD biomarker positive. pADi+ mild cognitive impairment patients (n = 63, 38%) were more likely to progress to AD dementia after 1 (odds ratio = 2.9) and 3 (odds ratio = 2.6) years.

Discussion: The pADi is a personalized, magnetic resonance imaging–derived AD biomarker that predicts progression to dementia.

© 2018 The Authors. Published by Elsevier Inc. on behalf of the Alzheimer's Association. This is an open access article under the CC BY-NC-ND license (http://creativecommons.org/licenses/by-nc-nd/4.0/).

Keywords: AD index; AD signature; Alzheimer's disease; Cortical thickness; Mild cognitive impairment

1. Background

Positron emission tomography (PET) and cerebrospinal fluid (CSF) biomarkers are the gold standard for identifying individuals with molecular evidence of Alzheimer's disease (AD) neuropathology, but these procedures are invasive (CSF), expensive (PET), and only accessible in specialized centers (PET) [1,2]. Magnetic resonance imaging (MRI), on the other hand, is noninvasive, less expensive, and more readily available than PET but less specific than amyloid PET or CSF to AD-related neurodegeneration. Although the magnitude of hippocampal atrophy in patients scanned in vivo and followed to autopsy correlates with the burden of neurofibrillary tangle pathology [3], hippocampal atrophy can also be seen in patients with a variety of neurodegenerative and other pathologies [4–6]. Spatial patterns of regional

brain atrophy measured by MRI may be sensitive to the typical localization of different types of neurodegenerative conditions, providing increased specificity [7]. For example, temporoparietal atrophy is strongly associated with the localization and magnitude of neurofibrillary tangles in AD [8,9], and in vivo tau PET investigations show a close correspondence between regional atrophy and tau PET signal [10–12]. However, the specificity of different cortical patterns of atrophy for AD pathology has received limited investigation [13].

Regional atrophy also shows clear relationships to the clinical characteristics of patients with neurodegenerative diseases [7,14,15]. Cortical thickness is a biologically meaningful measure interpretable with an MRI scan in an individual person that is highly reliable within and across scanner manufacturers, sequences, and field strengths [16]. We previously showed that a cortical thickness AD signature measure, comprised of nine regions of interest (ROIs), is a valid reflection of AD continuum severity and is reliable across multiple samples including those scanned at different field strengths [17]. Moreover, we have shown that it is associated with memory performance, cognitive decline, and progression to dementia [17–25], is a better predictor of progression from mild cognitive impairment (MCI) to AD compared to entorhinal [18] or hippocampal volume [24], and is closely associated with AD-like CSF characteristics [22].

One challenge associated with MRI-based biomarkers of neurodegenerative disease is that aging itself is associated with regional brain atrophy; we have shown that areas of prominent age-related cortical atrophy include regions partially overlapping with the AD signature [23,26–28]. Indeed, reducing the influence of age-related atrophy by adjusting the AD signature for these cortical changes resulted in increased correlation with CSF tau and amyloid β (Aβ) and better prediction than molecular markers of progression from MCI to dementia in 1 year [24].

Importantly, the cortical age-adjusted AD signature in our previous study was calculated as a residual from a group-level analysis. Therefore, while this study demonstrated the validity of a cortical age-adjusted AD signature MRI biomarker, the approach may not be generalizable to individual patients, potentially limiting its clinical applications. The goal of the present study was to calculate a cortical age-adjusted AD signature marker based on individual rather than group-level data and to identify a cut-point that could be used to classify individuals as high or low risk of likely harboring AD pathology based on CSF Aβ and tau. We chose to use a ratio of aging-signature cortical thickness to AD-signature cortical thickness because a ratio is more likely to be applicable across differences in scanners, sequences, or processing pipelines, and because this ratio can be interpreted as increasing likelihood of AD pathology with higher values.

With these motivations and this background in mind, we undertook this study hypothesizing that the "personalized AD cortical thickness index" (pADi) would discriminate patients with MCI who have molecular evidence of AD from MCI patients who likely do not have AD and that discrimination would be better than the AD signature alone (i.e., not adjusted for age-related cortical atrophy) or the aging signature. This would support the predictive pathological validity of this biomarker. We further hypothesized that a pADi cut-point derived from this MRI measure based on molecular biomarkers would predict progression from MCI to dementia with effect sizes similar to CSF biomarkers themselves, potentially supporting the use of this quantitative MRI measure probabilistically as a less expensive and invasive corollary of amyloid PET or CSF. This would support the predictive clinical validity of this biomarker.

2. Methods

The data and methods for biomarker (MRI, CSF) processing reported below are similar to those previously described in Dickerson and Wolk [24]. In addition, we provide a detailed analysis plan to test our hypotheses about an individualized MRI-derived, cortical age-adjusted AD biomarker, the pADi.

2.1. Participants

Data used in the preparation of this article were obtained from the Alzheimer's Disease Neuroimaging Initiative (ADNI) database (adni.loni.usc.edu). The ADNI was launched in 2003 as public-private partnership, led by Principal Investigator Michael W. Weiner, MD. The primary goal of ADNI has been to test whether serial MRI, PET, other biological markers and clinical and neuropsychological assessment can be combined to measure the progression of MCI and early AD.

For the current analysis, we selected individuals with a baseline diagnosis of MCI who had baseline CSF and MRI data available. Detailed diagnostic, inclusion, and exclusion criteria are described on the ADNI website (http://www.adni-info.org/). Methods for clinically characterizing patients as MCI or dementia have been described previously [29]; biomarkers were not used to facilitate the clinical diagnoses. "Conversion to AD Dementia" was defined as an ADNI diagnosis of AD dementia at follow-up assessments in patients who were initially classified as MCI at baseline.

2.2. Standard protocol approvals, registrations, and patient consents

Each participant gave written informed consent in accordance with institutional Human Subjects Research Committee guidelines.

2.3. MRI and analysis

We performed this analysis with a discovery sample and a validation sample. The discovery sample consisted of 149 MRI scans collected on a 3T scanner. One hundred ten of these 3T scans used a standardized magnetization prepared rapid acquisition gradient echo (MPRAGE) protocol on

Siemens scanner: sagittal plane, repetition time/time to echo/time for inversion (TR/TE/TI) 2300/2.98/900 ms, flip angle 9°, 25.6 cm field of view 240 × 256 in-plane matrix, 1.2 mm slice thickness. The remaining 39 3T scans used a standardized spoiled gradient recalled protocol on a GE scanner: sagittal plane, TR/TE/TI 6.984/2.84/400 ms, flip angle 11°, 26.0 cm field of view 256 × 256, 1.2 mm slice thickness. The independent validation sample consisted of 167 MRI scans collected on a 1.5T Siemens scanner using a standardized magnetization prepared rapid acquisition gradient echo protocol: sagittal plane, TR/TE/TI 2400/3/ 1000 ms, flip angle 8°, 24 cm field of view, 192 × 192 in-plane matrix, 1.2 mm slice thickness. Fully preprocessed scans were downloaded for analysis [30,31].

For both samples, T1 image volumes were examined quantitatively by a cortical surface-based reconstruction and analysis of cortical thickness, using a hypothesis-driven approach as described in multiple previous publications [17,18,23]. Briefly, we used nine ROIs (see Fig. 1) previously determined to be associated with AD, the "cortical signature" of AD. For the purposes of this study, we used a primary diagnostic biomarker, the single summary "AD signature measure," the average thickness of all nine ROIs. We also calculated a cortical signature of aging using eight ROIs where atrophy is seen primarily in normal aging with minimal additional effects of AD ("aging-only signature") [23]. We again calculated a single summary "aging-only signature measure" as the average thickness of these eight ROIs (Fig. 1). We calculated the pADi as the ratio of aging-only cortical thickness to AD-related cortical thickness scaled by a factor of 10 (i.e., [aging-only signature/AD signature] × 10). Thus, larger values indicate greater AD-related atrophy relative to aging-related atrophy, and values closer to or higher than 10 are considered more AD-like. There was no overlap between the current sample and the samples used to generate the AD [17] and aging [23] signatures.

To compare the pADi to a commonly used MRI biomarker in the field, we analyzed hippocampal volume using the measures provided by the automated segmentation procedure from FreeSurfer (summed across hemispheres) divided by total intracranial volume (ICV). We dichotomized ICV-corrected hippocampal volume for analysis based on a previously published threshold of 4.65 [32].

2.4. Baseline cerebrospinal fluid measures

We also examined baseline CSF levels of Aβ and phosphorylated tau (p-tau). We used previously published cut-point values [33] to classify participants as positive or negative for Aβ42 (Aβ42+ < 192), p-tau (p-tau+ > 23), and the ratio of p-tau to Aβ42 (p-tau/Aβ42 ratio + >0.10).

2.5. Statistical analysis

We performed receiver operating characteristic (ROC) curve analysis to determine how well the pADi discriminates
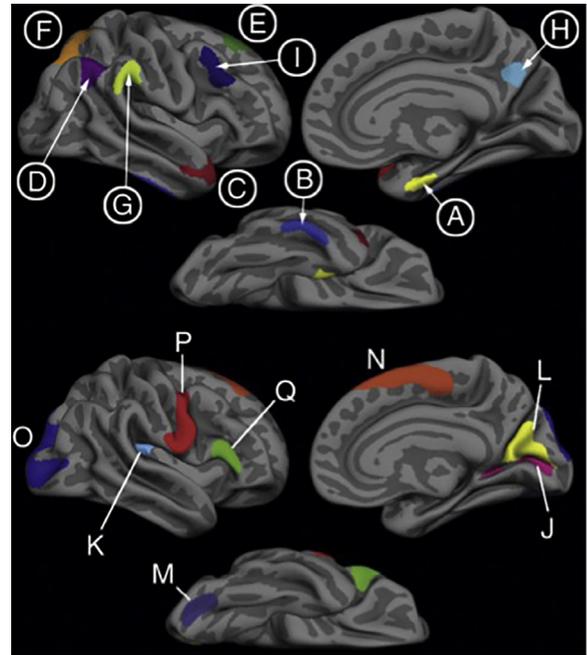
Fig. 1. AD signature and aging-only signature ROIs [23]. (Top) "AD signature" ROIs. Labels A, B, C, F, and H are AD-specific ROIs, where atrophy is seen primarily in AD. Labels D, E, G, and I are aging-AD overlap ROIs, where atrophy is seen in both aging and AD. (Bottom) "aging-specific" ROIs, where atrophy is seen primarily in normal aging with minimal additional effects of AD. Abbreviations: AD, Alzheimer's disease; ROI, region of interest; A, medial temporal; B, inferior temporal; C, temporal pole; D, angular; E, superior frontal; F, superior parietal; G, supramarginal; H, precuneus; I, middle frontal; J, calcarine; K, caudal insula; L, cuneus; M, caudal fusiform; N, dorsomedial frontal; O, lateral occipital; P, precentral; Q, inferior frontal.

MCI patients with and without molecular evidence of preclinical AD and to determine a cut-point to dichotomize the pADi based on this discrimination. Patients were stratified as being positive or negative for Aβ and p-tau based on cut-points described in Section 2.4. In the ROC analysis, we compared patients who were positive for both Aβ and p-tau (Aβ+/p-tau+) compared to patients who were negative for both Aβ and p-tau (Aβ−/p-tau−). Patients who were positive for either Aβ or p-tau but not both were excluded from the ROC analysis but not subsequent regression analyses.

For comparison, we repeated this ROC analysis using the AD signature and the aging-only signature instead of the pADi. We report area under the curve (AUC), which is an effective and combined measure of sensitivity and specificity that describes the inherent validity of a diagnostic test [34]. Our primary model was a parametric probit model fit with bootstrapping (1000 replications). We also performed analyses using maximum likelihood to test for robustness across different ROC approaches.

To investigate the clinical utility of the pADi to identify individuals with MCI who are at high or low risk of progressing to dementia, we developed cut-points based on three methods: the Liu method maximizes the product of the sensitivity and specificity and thus optimizes test discrimination [35]; the Youden method is defined as

"(sensitivity + specificity) − 1" and thus maximizes the ROC AUC [36,37]; and the nearest method finds the cut-point on the ROC curve closest to (0,1), that is, the point with perfect sensitivity and specificity. Because some studies may wish to optimize sensitivity or specificity (rather than both), we also report cut-points based on the value on the AUC curve closest to 90% sensitivity and 90% specificity.

We first performed the ROC analysis and cut-point determination in the Discovery 3T sample. We then replicated the analysis in the validation 1.5T sample to see if similar AUCs and cut-points were observed across data collected on scanners of different field strengths. Because a 3T scanner provides a stronger MRI signal, we then applied the cut-point derived in the discovery 3T sample to the data in the validation 1.5T sample for further analyses. To test the robustness of our findings, we repeated the ROC and cut-point analyses in the discovery 3T sample with alternative criteria for cases and controls using the well-established p-tau/Aβ42 ratio (p-tau/Aβ42 ratio+ vs. p-tau/Aβ42 ratio−; no patients were excluded).

We performed logistic regression with conversion to AD dementia as the outcome variable and the dichotomized pADi as the independent variable, controlling for age, sex, and education. We examined conversion to AD dementia by 1-year and 3-year follow-up. We report the effect sizes (odds ratio [OR]) to models using dichotomized ICV-corrected hippocampal volume and CSF biomarkers for Aβ, p-tau, and p-tau/Aβ42 for comparison. Finally, we examined a model with dichotomized variables for pADi, p-tau, and Aβ42 simultaneously to see if the pADi adds predictive value in models that already account for molecular evidence of AD pathology.

To be as inclusive as possible initially, we included all individuals meeting a clinical diagnosis of AD dementia at the follow-up in our main logistic regression analysis. However, several of the identified converters did not have CSF biomarker evidence of AD (elevated Aβ and/or tau) at baseline, suggesting that they may have had dementia due to another cause other than AD, despite their clinical diagnosis. Unfortunately, not all of these participants had CSF biomarker data available at the 1- and 3-year assessments, so it is not known if these patients progressed to biomarker positivity (coinciding with their transition to AD dementia), despite being biomarker negative at baseline. Therefore, we performed two sensitivity analyses: the first excluded all patients who were negative for CSF Aβ and/or tau at baseline but converted to dementia at the follow-up (regardless of whether they had biomarker data available at the 1- and 3-year visits); the second excluded only those patients who converted to dementia who also had a known biomarker-negative status at the follow-up.

3. Results

Baseline characteristics of the two samples are described in Table 1.

The ROC results were similar using either the maximum likelihood or bootstrapping approaches; bootstrapping yielded slightly higher AUCs and provided bias-corrected 95% confidence intervals (CIs) and so are reported and displayed in Fig. 2. The AUC for the ROC analysis of pADi discriminating MCI Aβ+/p-tau+ from MCI Aβ−/p-tau− was 0.69 and 0.72 for the discovery 3T and validation 1.5T samples, respectfully. This is roughly equivalent to a Cohen's d of 0.7 or a point biserial correlation coefficient of 0.4 and thus constitutes a moderate effect size [38] and good diagnostic accuracy [39]. The pADi had a higher AUC than either the AD signature or the aging-only signature. However, statistical tests for the equality of the ROC areas between the pADi and the AD and aging signatures revealed that the pADi AUC was significantly higher compared to the aging Signature in the 1.5 sample (χ^2 = 7.9, P = .005) but not the 3T sample (χ^2 = 3.4, P = .066), and that the differences between the pADi and the AD signature were not statistically significant in either sample (1.5T: χ^2 = 1.8, P = .18; 3T: χ^2 = 0.5, P = .45).

The Liu, Youden, and nearest methods all identified a cut-point of 8.69 in the discovery 3T sample and 8.65 in the validation 1.5T sample. Cut-points corresponding to 90% sensitivity and 90% specificity were 8.44 and 9.03, respectively, in the discovery 3T sample; these values were 8.23 and

Table 1
Sample characteristics

Sample characteristic	Discovery 3T sample (N = 149)	Validation 1.5 T sample (N = 167)
Age, years; mean (SD)	71.44 (7.3)	74.4 (7.5)
Sex, female; n (%)	71 (48)	58 (35)
Education, years; mean (SD)	16.2 (2.7)	15.6 (3.1)
APOE4+; n (%)	64 (45)	93 (56)
MMSE; mean (SD)	28.2 (1.6)	26.9 (1.8)
CSF p-tau; mean (SD)	25.61 (14.6)	36.3 (18.7)
CSF p-tau+; n (%)	70 (47)	117 (70.1)
CSF Aβ42; mean (SD)	216.7 (74.4)	163.1 (53.2)
CSF Aβ42+; n (%)	64 (43)	124 (74.3)
CSF p-tau/Aβ42 ratio; mean (SD)	0.15 (0.12)	0.27 (0.19)
CSF p-tau/Aβ42 ratio+; n (%)	76 (51)	131 (78.4)
Adjusted hippocampal volume; mean (SD)	4.85 (0.73)	4.07 (0.56)
Adjusted hippocampal volume+; n (%)	62 (42)	144 (86)
AD signature, mm; mean (SD)	2.57 (0.13)	2.43 (0.16)
Aging-only signature, mm; mean (SD)	2.24 (0.08)	2.07 (0.11)
Personalized AD cortical thickness index (pADi); mean (SD)	8.73 (0.34)	8.56 (0.33)
AD by 1-year follow-up; n/N (%)*	N/A	30/155 (19)
AD by 3-year follow-up; n/N (%)*	N/A	73/135 (54)

Abbreviations: AD, Alzheimer's disease; Adjusted hippocampal volume, bilateral hippocampal volume corrected for intracranial volume; APOE, apolipoprotein E; CSF, cerebrospinal fluid; MMSE, Mini Mental State Examination; p-tau, phosphorylated tau; SD, standard deviation.

*Progression to AD was assessed in the validation 1.5 T sample only; progression to AD by 1-year follow-up was assessed in the n = 155 who developed AD by or were followed for at least 1 year; progression to AD by 3-year follow-up was assessed in the N = 135 who developed AD by or were followed for at least 3 years.
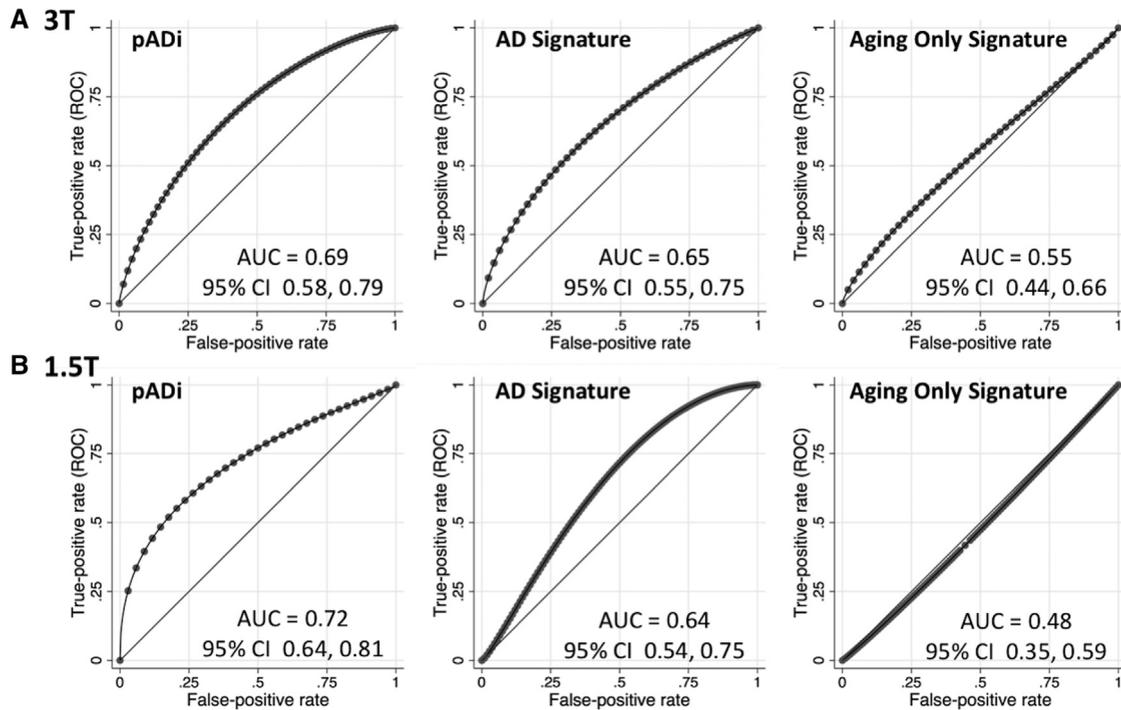
Fig. 2. ROC curves for discriminating MCI patients with and without molecular evidence of AD (Aβ+/p-tau+ vs. Aβ−/p-tau−). ROC curves are displayed for the pADi (left), the AD signature (middle), and the aging-only signature (right) for the discovery 3T sample (A, top) and validation 1.5T sample (B, bottom). AUC and bias-corrected 95% CIs are reported for each curve and a fit line (AUC = 0.50) is displayed for reference. X-axis: false-positive rate; Y-axis: true-positive rate (ROC). Abbreviations: AD, Alzheimer's disease; AUC, area under the curve; CIs, confidence intervals; ROC, receiver operating characteristic; MCI, mild cognitive impairment; pADi, personalized AD cortical thickness index.

8.71 in the validation 1.5T sample. Sensitivity, specificity, percent correctly classified, and positive and negative likelihood ratios for the cut-points are provided in Table 2 [40].

When we instead classified patients based on positivity of the p-tau/Aβ42 ratio in the discovery 3T sample, results were consistent with those observed in our primary analysis: the AUCs for the pADi, AD signature, and aging signature were 0.69, 0.60, and 0.50, respectively. Furthermore, the cut-point analysis using the p-tau/Aβ42 ratio identified the same cut-point as our primary analysis (8.69) using the

Liu and nearest methods, while the Youden method identified 8.55 as the optimal cut-point. These findings provide further confidence in the clinical utility of the cut-point of 8.69 for our subsequent validation analyses.

Next, we dichotomized patients in the validation 1.5T sample based on three cut-points derived from our primary analysis in the discovery 3T sample: the cut-points for 90% sensitivity, 90% specificity, and the three empirical methods. The sensitivity cut-point of 8.44 derived in the discovery 3T sample identified 97/167 (58%) MCI patients in

Table 2
Empirical estimation of cut-point from ROC analysis

Method	Cut-point	95% CI	Sensitivity at cut-point	Specificity at cut-point	Percent correctly classified	LR+	LR−
Discovery 3 T sample							
Liu	8.69	8.56, 8.82	0.69	0.62	65	1.85	0.49
Youden	8.69	8.45, 8.93	0.69	0.62	65	1.85	0.49
Nearest	8.69	8.58, 8.80	0.69	0.62	65	1.85	0.49
90% Sensitivity	8.44	N/A	0.90	0.22	51	1.15	0.47
90% Specificity	9.03	N/A	0.27	0.89	62	2.43	0.82
Validation 1.5T sample							
Liu	8.65	8.37, 8.94	0.52	0.88	61	4.41	0.55
Youden	8.65	8.40, 8.91	0.52	0.88	61	4.41	0.55
Nearest	8.65	8.41, 8.90	0.52	0.88	61	4.41	0.55
90% Sensitivity	8.23	N/A	0.90	0.26	75	1.22	0.39
90% Specificity	8.71	N/A	0.48	0.91	58	5.46	0.57

Abbreviations: CI, confidence interval; ROC, receiver operating characteristic.

NOTE. LR+ = Positive likelihood ratio; a LR+ greater than one indicates the cut-point is associated with the disease state; larger values indicate better diagnostic accuracy. LR− = Negative likelihood ratio; a LR− less than one (0–1) indicates the cut-point is associated with absence of the disease state; smaller values indicate better diagnostic accuracy.
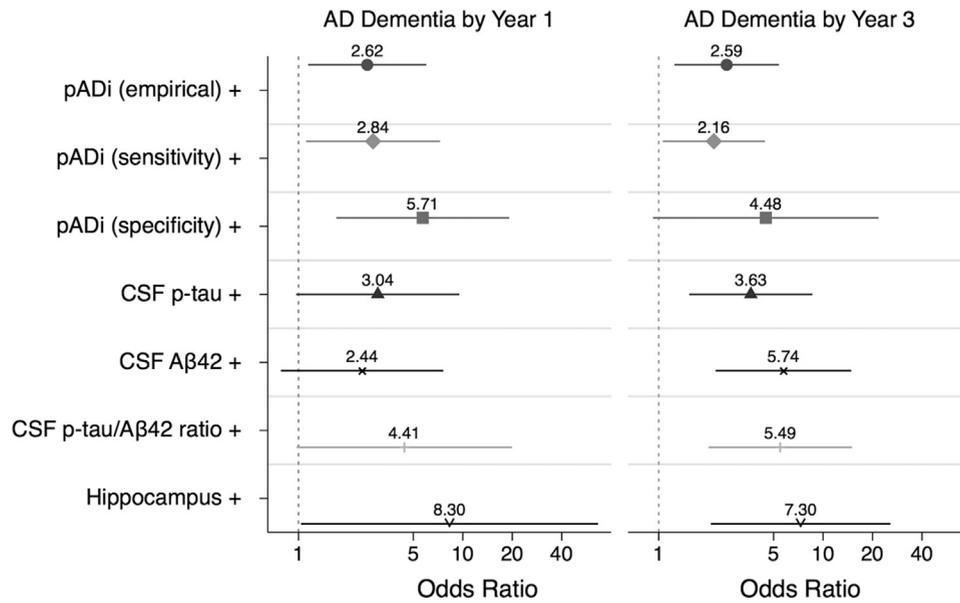
Fig. 3. Odds of progressing to AD dementia by 1-year (left) or 3-year (right) follow-up. Odds ratios and 95% confidence intervals (horizontal bar) are displayed for each the dichotomized biomarkers of interest on the y-axis on a logarithmic scale. The dashed referenced line is displayed at odds ratio = 1. Hippocampus and CSF biomarker cut-points were based on previously published thresholds. Abbreviations: AD, Alzheimer's disease; CSF, cerebrospinal fluid; pADi, personalized AD cortical thickness index (dichotomized by one of three methods indicated in the parentheses).

the validation 1.5T sample as pADi+; the specificity cut-point of 9.03 derived in the discovery 3T sample identified 13 (8%) in the validation 1.5T sample as pADi+; and the empirical cut-point of 8.69 derived in the discovery 3T sample identified 63 (38%) of the validation 1.5T sample as pADi+. Of those MCI patients who were pADi+, 73% (71/97) were positive for both CSF Aβ42 and p-tau using the sensitivity cut-point, 77% (10/13) were positive for both using the specificity cut-point, and 83% (52/63) were positive using the empirical cut-point.

pADi positivity by all three cut-points predicted conversion to AD dementia by a 1-year follow-up, but only the empirical cut-point and the sensitivity cut-point predicted progression to AD dementia by a 3-year follow-up (Table 3, Fig. 3). In contrast, the CSF biomarkers did not predict conversion by 1-year follow-up but did predict conversion by 3-year follow-up (Table 3, Fig. 3). ICV-corrected hippocampal volume predicted AD by a 1- and 3-year follow-up, but CIs were large, likely because the vast majority of patients in the 1.5T test sample were

Table 3
Odds of progressing from MCI to AD dementia in the validation 1.5T sample

Biomarker (dichotomous)	N (%) positive	Odds ratio	Confidence interval	*P* value	Pseudo R^2
1-year follow-up (N = 156)					
pADi (empirical)+	60 (39%)	2.90	1.37, 6.63	.011	0.07
pADi (sens)+	90 (58%)	3.12	1.22, 8.00	.018	0.07
pADi (spec)+	13 (8%)	5.57	1.64, 18.85	.006	0.08
p-tau+	110 (71%)	2.41	0.83, 6.97	.10	0.05
Aβ42+	115 (74%)	1.91	0.67, 5.49	.23	0.04
p-tau/Aβ42 ratio+	122 (79%)	2.89	0.80, 10.46	.11	0.05
Hippocampus+	133 (86%)	8.30	1.03, 66.52	.046	0.07
3-year follow-up (N = 136)					
pADi (empirical)+	55 (41%)	2.59	1.25, 5.39	.011	0.06
pADi (sens)+	80 (59%)	2.16	1.06, 4.43	.034	0.05
pADi (spec)+	12 (9%)	4.48	0.92, 21.75	.063	0.05
p-tau+	101 (75%)	3.63	1.53, 8.61	.003	0.07
Aβ42+	104 (77%)	5.73	2.22, 14.82	<.001	0.10
p-tau/Aβ42 ratio+	108 (80%)	5.48	2.01, 14.99	.001	0.09
Hippocampus+	117 (87%)	7.30	2.08, 25.70	.002	0.09

Abbreviations: AD, Alzheimer's disease; CSF, cerebrospinal fluid; MCI, mild cognitive impairment; pADi, personalized AD cortical thickness index.

NOTE. pADi cut-points were derived in the discovery 3T sample. Empirical cut-point = the average cut-point across three methods (Liu, Youden, and nearest); patients were classified as being pADi+ if their pADi was greater than or equal to 8.69. Sens = 90% sensitivity cut-point; patients were classified as being pADi+ if their pADi was greater than or equal to 8.44. Spec = 90% specificity cut-point; patients were classified as being pADi+ if their pADi was greater than or equal to 9.03. Hippocampus and CSF biomarker cut-points were based on previously published thresholds.

classified as hippocampus+, including 77% of patients who remained stable over 3 years. Sensitivity analyses excluding patients who converted to dementia but who lacked CSF biomarker evidence of AD at baseline or follow-up yielded similar results for the three dichotomous pADi variables, suggesting that these patients were not strongly influencing our main results.

Finally, we investigated whether pADi positivity would add predictive value to models that also included p-tau and Aβ42 positivity. Because p-tau+ and Aβ42+ did not significantly predict progression to AD at a 1-year follow-up, we investigated this combined model for 3-year follow-up only and focused on the empirical cut-point. In the combined model, only Aβ42+ (OR = 3.76, 95% CI [1.21, 11.71], P = .022) but not p-tau+ (OR = 1.56, 95% CI [0.54, 4.54], P = .42) or pADi+ (OR = 1.96, 95% CI [0.91, 4.25], P = .088) predicted progression to AD by a 3-year follow-up. However, this combined model had higher pseudo R^2 (0.13) than any of the models with a single biomarker, and the pseudo R^2-change after adding pADi into the combined model was 0.016 compared to 0.030 for Aβ42 and 0.004 for p-tau.

4. Discussion

The pADi is an MRI-derived, brain-age-adjusted AD biomarker that can discriminate MCI patients with molecular markers of AD (CSF Aβ+/p-tau+) from those without (CSF Aβ−/p-tau−) with good diagnostic accuracy and (although not statistically different) larger AUCs than either the AD or aging-only cortical signatures, supporting the predictive pathological validity of this biomarker. Importantly, our results were consistent across two well-characterized samples of MCI patients with MRI data collected on scanners of two different field strengths. The optimal cut-point across three empirical methods of 8.69 had a moderate AUC effect size and good diagnostic accuracy. Moreover, pADi positivity outperformed CSF biomarkers (p-tau+/−, Aβ42+/−, p-tau/ Aβ42 ratio+/−) in predicting odds of progressing to AD dementia over 1 year, supporting the predictive clinical validity of the pADi biomarker. CSF biomarker positivity had higher ORs than the pADi for predicting progression to dementia due to AD over 3 years, but the pADi performed in a similar range as p-tau. In a combined model with dichotomous predictors for AD-index, p-tau, and Aβ42, only Aβ42 positivity significantly predicted conversion to AD dementia by 3-year follow-up, but inclusion of pADi improved the model. Together, these results suggest that the pADi is a useful MRI biomarker that can identify MCI likely due to AD in individual patients. The pADi may even be a better prognosticator than CSF biomarkers for shorter intervals (e.g., ≤1 year) in some populations (e.g., MCI).

The pADi represents an individualized measure of cortical atrophy in a pattern suggestive of AD pathology, scaled by the amount of age-related brain atrophy. While many studies have previously shown that the AD signature is a valuable

biomarker in predicting important clinical outcomes [17–19,22,23], this study suggests that it may perform better if adjusted for an estimate of cortical age. Moreover, as these models included chronological age as a covariate, the current findings suggest that adjusting for "brain age," beyond chronological age, is important in enhancing diagnostic and prognostic precision. Although the regional pattern of atrophy measureable by MRI and associated with AD varies as a function of age [41], this pattern is probabilistically associated with AD neuropathology—particularly neurofibrillary tau pathology [12]. We showed that the pADi is better at discriminating MCI patients with AD pathology from MCI patients without AD pathology than the AD signature itself, supporting our theory that the pADi is more specific to AD than the AD signature without adjustment for cortical age.

Previous studies have also shown that an age-corrected AD signature [24] and the uncorrected AD signature [18] are better (continuous) predictors of progression to AD dementia than other regional atrophy measures like hippocampal volume. In this study, hippocampus positivity was associated with larger OR point estimates compared to pADi positivity for both the 1- and 3-year follow-up, but also much larger CIs, suggesting greater variability in the measurement; as a result, z-values were larger for all three pADi cut-points compared to hippocampal volume for conversion to AD dementia by 1 year. It is important to note that unlike cortical thickness, hippocampal volumes may be biased by different scanners and field strengths [42] and scale with head size, which are in turn related to sex [43]. For these reasons, our group and others [44] prefer to use cortical thickness measures over brain volumes when possible.

The aging-only signature, which comprises brain regions where atrophy is seen primarily in normal aging with minimal additional effects of AD, performed equivalently to a random classification model, and thus has poor diagnostic accuracy for AD. That is, measures that include these regions are likely adding noise to the analysis. Importantly, unlike our previous study [24], which relied on group-level regression data to derive an age-adjusted biomarker, the pADi can be calculated in an individual patient without relying on group data that may be less generalizable. Indeed, the extension of this approach to individuals drawing on ratios of regional cortical thickness measures provides an opportunity to examine the generalizability of this type of measure to MRI data collected using different instrumentation. Our study showed that the pADi is relatively consistent across scanners of different field strengths, and that the index derived from data collected on a 3T scanner (our discovery sample) can be applied to data collected on a 1.5 scanner (our validation sample).

We further extended our previous work by dichotomizing the cortical thickness biomarker based on multiple types of cut-point criteria. Our results showed that an empirically derived cut-point to dichotomize the pADi has good predictive ability for progression to AD over the short (1 year) and longer (3 years) term. These results suggest that the pADi could be

useful for screening MCI patients into AD clinical trials, particularly for trials with designs aiming to enroll patients expected to progress at a relatively more rapid rate. Furthermore, because cortical thickness has been shown to be highly reliable within and across scanner manufacturers, sequences, and field strengths [16], the pADi is expected to perform robustly in multicenter trials, which we plan to study directly.

Finally, our analysis with dichotomous predictors for pADi, p-tau, and Aβ42 in a single model showed that Aβ was the strongest predictor of progression to AD dementia over three years, but that model fit was higher in the combined model than models with the individual biomarkers. Although our sample was too small to investigate the recently proposed A/T/N framework directly [45], this model provides evidence that the dichotomized pADi could be useful as a measure for neurodegeneration (N+/−) in models with biomarkers for amyloid (A+/−) and tau (T+/−). Further investigation should illuminate the specificity of the pADi to AD pathology versus other neurodegenerative pathologies because we need methods to help differentiate various neurodegenerative pathologies while we work toward the development of specific molecular biomarkers for the entire family of neurodegenerative diseases.

ROC analysis is a common approach in biomarker research to derive cut-points [46]. We evaluated three methods for maximizing sensitivity and specificity from an ROC analysis, all of which identified the same cut-point (within each sample). However, other criteria to define cut-points are worth consideration. For instance, Jack et al. [44] recently recommended that cut-points for cortical thickness be based on the accuracy of discriminating cognitively impaired versus young cognitively normal controls (or vs. age-matched cognitively normal controls for a more conservative estimate); this approach aims to discriminate people with preclinical AD from those with age-related atrophy. In contrast, we chose a cut-point that best differentiated MCI patients with and without molecular biomarkers of AD. These populations were selected for our study because the etiology of MCI is variable and can be due to a number of causes including degenerative, vascular, depressive, traumatic, medical comorbidities, or mixed disease. Patients meeting the core clinical criteria for MCI who also have positive biomarkers for both Aβ and neuronal injury (e.g., CSF Aβ+ and p-tau+) have the highest level of certainty for "MCI due to AD" and progression to AD dementia over time; in contrast, MCI patients who have negative biomarkers for both Aβ and neuronal injury (e.g., CSF Aβ− and p-tau−) are considered to have the lowest likelihood of underlying AD pathophysiology [47]. Thus, our approach was chosen to optimize a cut-point that discriminates high likelihood of AD and high progression to dementia from low likelihood of AD and low likelihood of progression to dementia. Because the selected cut-point was optimized in an MCI sample, it is possible that other cut-points may be more appropriate

for different samples including those representing the preclinical phase of AD or with richer racial, ethnic, and socioeconomic diversity. Because ADNI may not be representative of the heterogeneous populations seen in the clinic and in large clinical trials, it will be important to replicate these analyses in other samples.

Although the pADi has good diagnostic accuracy, using the recommended cut-point will still incorrectly classify some patients. Incorrect classification may in part be due to heterogeneity of atrophy within the AD spectrum [48,49]. Currently, the pADi is based on a single, noninvasive imaging modality that is relatively widely available and largely fully automated; but this index could be refined as technological and computational developments make it possible to measure subtler features of brain atrophy and account for intersubject variability. Even with these limitations in mind, this study provides support for the use of the pADi as an MRI-derived AD biomarker than can be interpreted in individual patients and which has relevance for predicting both pathology and clinical outcomes.

RESEARCH IN CONTEXT

1. Systematic review: The authors reviewed the literature using traditional (e.g., PubMed) sources and meeting abstracts and presentations. Multiple previous studies have investigated magnetic resonance imaging–derived Alzheimer's disease (AD) biomarkers and signatures, which are appropriately cited.

2. Interpretation: The personalized AD cortical thickness index is a magnetic resonance imaging–derived, brain-age-adjusted AD biomarker that can discriminate patients with molecular markers of AD from those without. We recommend a cut-point for dichotomizing the personalized AD cortical thickness index that identifies mild cognitive impairment likely due to AD in individual patients.

3. Future directions: Our results were consistent across two well-characterized samples of mild cognitive impairment patients, but additional studies are needed to determine generalizability to other populations. Future studies may also include using the personalized AD cortical thickness index to categorize large populations into classification schemes for AD biomarkers to enrich for clinical trials or research studies or to identify patients at high risk for AD dementia who may be candidates for additional biomarker testing or interventions.

References

[1] Sperling RA, Aisen PS, Beckett LA, Bennett DA, Craft S, Fagan AM, et al. Toward defining the preclinical stages of Alzheimer's disease: recommendations from the National Institute on Aging-Alzheimer's Association workgroups on diagnostic guidelines for Alzheimer's disease. Alzheimers Dement 2011;7:280–92.

[2] Dubois B, Hampel H, Feldman HH, Scheltens P, Aisen P, Andrieu S, et al. Preclinical Alzheimer's disease: definition, natural history, and diagnostic criteria. Alzheimers Dement 2016;12:292–323.

[3] Jack CR Jr, Dickson DW, Parisi JE, Xu YC, Cha RH, O'Brien PC, et al. Antemortem MRI findings correlate with hippocampal neuropathology in typical aging and dementia. Neurology 2002;58:750–7.

[4] Laakso MP, Partanen K, Riekkinen P, Lehtovirta M, Helkala EL, Hallikainen M, et al. Hippocampal volumes in Alzheimer's disease, Parkinson's disease with and without dementia, and in vascular dementia: an MRI study. Neurology 1996;46:678–81.

[5] Onyike CU, Pletnikova O, Sloane KL, Sullivan C, Troncoso JC, Rabins PV. Hippocampal sclerosis dementia: an amnesic variant of frontotemporal degeneration. Dement Neuropsychol 2013;7:83–7.

[6] Sheline YI, Wang PW, Gado MH, Csernansky JG, Vannier MW. Hippocampal atrophy in recurrent major depression. Proc Natl Acad Sci U S A 1996;93:3908–13.

[7] Harper L, Bouwman F, Burton EJ, Barkhof F, Scheltens P, O'Brien JT, et al. Patterns of atrophy in pathologically confirmed dementias: a voxelwise analysis. J Neurol Neurosurg Psychiatry 2017;88:908–16.

[8] Whitwell JL, Dickson DW, Murray ME, Weigand SD, Tosakulwong N, Senjem ML, et al. Neuroimaging correlates of pathologically defined subtypes of Alzheimer's disease: a case-control study. Lancet Neurol 2012;11:868–77.

[9] Whitwell JL, Josephs KA, Murray ME, Kantarci K, Przybelski SA, Weigand SD, et al. MRI correlates of neurofibrillary tangle pathology at autopsy: a voxel-based morphometry study. Neurology 2008;71:743–9.

[10] Ossenkoppele R, Schonhaut DR, Scholl M, Lockhart SN, Ayakta N, Baker SL, et al. Tau PET patterns mirror clinical and neuroanatomical variability in Alzheimer's disease. Brain 2016;139:1551–67.

[11] LaPoint MR, Chhatwal JP, Sepulcre J, Johnson KA, Sperling RA, Schultz AP. The association between tau PET and retrospective cortical thinning in clinically normal elderly. Neuroimage 2017; 157:612–22.

[12] Xia C, Makaretz SJ, Caso C, McGinnis S, Gomperts SN, Sepulcre J, et al. Association of in vivo [18F]AV-1451 tau PET imaging results with cortical atrophy and symptoms in typical and atypical Alzheimer disease. JAMA Neurol 2017;74:427–36.

[13] Rabinovici GD, Seeley WW, Kim EJ, Gorno-Tempini ML, Rascovsky K, Pagliaro TA, et al. Distinct MRI atrophy patterns in autopsy-proven Alzheimer's disease and frontotemporal lobar degeneration. Am J Alzheimers Dis Other Demen 2007;22:474–88.

[14] Park JY, Na HK, Kim S, Kim H, Kim HJ, Seo SW, et al. Robust Identification of Alzheimer's Disease subtypes based on cortical atrophy patterns. Sci Rep 2017;7:43270.

[15] Noh Y, Jeon S, Lee JM, Seo SW, Kim GH, Cho H, et al. Anatomical heterogeneity of Alzheimer disease: based on cortical thickness on MRIs. Neurology 2014;83:1936–44.

[16] Dickerson BC, Fenstermacher E, Salat DH, Wolk DA, Maguire RP, Desikan R, et al. Detection of cortical thickness correlates of cognitive performance: reliability across MRI scan sessions, scanners, and field strengths. Neuroimage 2008;39:10–8.

[17] Dickerson BC, Bakkour A, Salat DH, Feczko E, Pacheco J, Greve DN, et al. The cortical signature of Alzheimer's disease: regionally specific cortical thinning relates to symptom severity in very mild to mild AD dementia and is detectable in asymptomatic amyloid-positive individuals. Cereb Cortex 2009;19:497–510.

[18] Bakkour A, Morris JC, Dickerson BC. The cortical signature of prodromal AD: regional thinning predicts mild AD dementia. Neurology 2009;72:1048–55.

[19] Dickerson BC, Stoub TR, Shah RC, Sperling RA, Killiany RJ, Albert MS, et al. Alzheimer-signature MRI biomarker predicts AD dementia in cognitively normal adults. Neurology 2011;76:1395–402.

[20] Dickerson BC, Wolk DA. Alzheimer's Disease Neuroimaging I. Dysexecutive versus amnesic phenotypes of very mild Alzheimer's disease are associated with distinct clinical, genetic and cortical thinning characteristics. J Neurol Neurosurg Psychiatry 2011;82:45–51.

[21] Putcha D, Brickhouse M, O'Keefe K, Sullivan C, Rentz D, Marshall G, et al. Hippocampal hyperactivation associated with cortical thinning in Alzheimer's disease signature regions in non-demented elderly adults. J Neurosci 2011;31:17680–8.

[22] Dickerson BC, Wolk DA. Alzheimer's Disease Neuroimaging I. MRI cortical thickness biomarker predicts AD-like CSF and cognitive decline in normal adults. Neurology 2012;78:84–90.

[23] Bakkour A, Morris JC, Wolk DA, Dickerson BC. The effects of aging and Alzheimer's disease on cerebral cortical anatomy: specificity and differential relationships with cognition. Neuroimage 2013; 76:332–44.

[24] Dickerson BC, Wolk DA. Alzheimer's Disease Neuroimaging I. Biomarker-based prediction of progression in MCI: Comparison of AD signature and hippocampal volume with spinal fluid amyloid-beta and tau. Front Aging Neurosci 2013;5:55.

[25] Busovaca E, Zimmerman ME, Meier IB, Griffith EY, Grieve SM, Korgaonkar MS, et al. Is the Alzheimer's disease cortical thickness signature a biological marker for memory? Brain Imaging Behav 2016;10:517–23.

[26] Habes M, Janowitz D, Erus G, Toledo JB, Resnick SM, Doshi J, et al. Advanced brain aging: relationship with epidemiologic and genetic risk factors, and overlap with Alzheimer disease atrophy patterns. Transl Psychiatry 2016;6:e775.

[27] Salat DH, Buckner RL, Snyder AZ, Greve DN, Desikan RS, Busa E, et al. Thinning of the cerebral cortex in aging. Cereb Cortex 2004; 14:721–30.

[28] Fjell AM, McEvoy L, Holland D, Dale AM, Walhovd KB, Alzheimer's Disease Neuroimaging I. What is normal in normal aging? Effects of aging, amyloid and Alzheimer's disease on the cerebral cortex and the hippocampus. Prog Neurobiol 2014;117:20–40.

[29] Petersen RC, Aisen PS, Beckett LA, Donohue MC, Gamst AC, Harvey DJ, et al. Alzheimer's Disease Neuroimaging Initiative (ADNI): clinical characterization. Neurology 2010;74:201–9.

[30] Jack CR Jr, Bernstein MA, Fox NC, Thompson P, Alexander G, Harvey D, et al. The Alzheimer's Disease Neuroimaging Initiative (ADNI): MRI methods. J Magn Reson Imaging 2008;27:685–91.

[31] Jack CR Jr, Barnes J, Bernstein MA, Borowski BJ, Brewer J, Clegg S, et al. Magnetic resonance imaging in Alzheimer's Disease Neuroimaging Initiative 2. Alzheimers Dement 2015;11:740–56.

[32] Schreiber S, Schreiber F, Lockhart SN, Horng A, Bejanin A, Landau SM, et al. Alzheimer disease signature neurodegeneration and APOE genotype in mild cognitive impairment with suspected non-Alzheimer disease pathophysiology. JAMA Neurol 2017; 74:650–9.

[33] Shaw LM, Vanderstichele H, Knapik-Czajka M, Clark CM, Aisen PS, Petersen RC, et al. Cerebrospinal fluid biomarker signature in Alzheimer's disease neuroimaging initiative subjects. Ann Neurol 2009; 65:403–13.

[34] Hajian-Tilaki K. Receiver operating characteristic (ROC) curve analysis for medical diagnostic test evaluation. Caspian J Intern Med 2013; 4:627–35.

[35] Liu X. Classification accuracy and cut point selection. Stat Med 2012; 31:2676–86.

[36] Youden WJ. Index for rating diagnostic tests. Cancer 1950;3:32–5.

[37] Fluss R, Faraggi D, Reiser B. Estimation of the Youden Index and its associated cutoff point. Biom J 2005;47:458–72.

[38] Rice ME, Harris GT. Comparing effect sizes in follow-up studies: ROC Area, Cohen's d, and r. Law Hum Behav 2005;29:615–20.

[39] Simundic AM. Measures of diagnostic accuracy: basic definitions. EJIFCC 2009;19:203–11.

[40] Deeks JJ, Altman DG. Diagnostic tests 4: likelihood ratios. BMJ 2004; 329:168–9.

[41] Dickerson BC, Brickhouse M, McGinnis S, Wolk DA. Alzheimer's disease: the influence of age on clinical heterogeneity through the human brain connectome. Alzheimers Dement (Amst) 2017;6:122–35.

[42] Jovicich J, Czanner S, Han X, Salat D, van der Kouwe A, Quinn B, et al. MRI-derived measurements of human subcortical, ventricular and intracranial brain volumes: Reliability effects of scan sessions, acquisition sequences, data analyses, scanner upgrade, scanner vendors and field strengths. Neuroimage 2009;46:177–92.

[43] Barnes J, Ridgway GR, Bartlett J, Henley SM, Lehmann M, Hobbs N, et al. Head size, age and gender adjustment in MRI studies: a necessary nuisance? Neuroimage 2010;53:1244–55.

[44] Jack CR Jr, Wiste HJ, Weigand SD, Therneau TM, Lowe VJ, Knopman DS, et al. Defining imaging biomarker cut points for brain aging and Alzheimer's disease. Alzheimers Dement 2017;13:205–16.

[45] Jack CR Jr, Bennett DA, Blennow K, Carrillo MC, Feldman HH, Frisoni GB, et al. A/T/N: An unbiased descriptive classification scheme for Alzheimer disease biomarkers. Neurology 2016; 87:539–47.

[46] Looney SW, Hagan JL. Analysis of biomarker data: a practical guide. Hoboken, New Jersey: John Wiley & Sons, Inc.; 2015.

[47] Albert MS, DeKosky ST, Dickson D, Dubois B, Feldman HH, Fox NC, et al. The diagnosis of mild cognitive impairment due to Alzheimer's disease: recommendations from the National Institute on Aging-Alzheimer's Association workgroups on diagnostic guidelines for Alzheimer's disease. Alzheimers Dement 2011;7:270–9.

[48] Coutu JP, Lindemer ER, Konukoglu E, Salat DH, Alzheimer's Disease Neuroimaging I. Two distinct classes of degenerative change are independently linked to clinical progression in mild cognitive impairment. Neurobiol Aging 2017;54:1–9.

[49] Dong A, Toledo JB, Honnorat N, Doshi J, Varol E, Sotiras A, et al. Heterogeneity of neuroanatomical patterns in prodromal Alzheimer's disease: links to cognition, progression and biomarkers. Brain 2017; 140:735–47.